Integrating environmental gradients into breeding: application of genomic reactions norms in a perennial species

Victor Papin, Alexandre Bosc, Leopoldo Sanchez, Laurent Bouffier

Title page

Title: Integrating environmental gradients into breeding: application of genomic reactions norms in a perennial species

Full names of all authors and their affiliations:

Victor Papin[1], Alexandre Bosc[2], Leopoldo Sanchez[3*] and Laurent Bouffier[1*]

[1] : INRAE, BIOGECO, UMR 1202, 69 route d'Arcachon, 33610 Cestas, France. University of Bordeaux, BIOGECO, UMR 1202, 33400 Talence, France.

[2] : INRAE, UMR 1391 ISPA, 71 Avenue Edouard Bourlaux, 33140 Villenave-d'Ornon, France. Bordeaux Sciences Agro, 1 cours du Général de Gaulle 33170 Gradignan, France.

[3] : INRAE-ONF, BioForA, UMR 0588, 2163 Avenue de la Pomme de Pin, CS 40001 Ardon, 45075, Cedex 2, Orléans, France.

*: these authors contributed equally to this work

Corresponding author: Laurent Bouffier - laurent.bouffier@inrae.fr

Word count: 6672 words (From the beginning of the introduction to the end of the discussion)

Abstract

Global warming threatens the productivity of forest plantations. We propose here the integration of environmental information into a genomic evaluation scheme using individual reaction norms, to enable the quantification of resilience in forest tree improvement and conservation strategies in the coming decades. Random regression models were used to fit wood ring series, reflecting the longitudinal phenotypic plasticity of tree growth, according to various environmental gradients. The prediction accuracy of the models was considered to select the most relevant environmental gradient, namely a gradient derived from an ecophysiological model and combining trunk water potential and temperature. Even if the individual ranking was preserved over most of the environmental gradient, strong genotype x environment interactions were detected in the extreme unfavorable part of the gradient, which includes environmental conditions that are very likely to be more frequent in the future. Combining genomic information and longitudinal data allowed to predict the growth of individuals in environments where they have not been observed. Phenotyping of 50% of the individuals in all the environments studied allowed to predict the growth of the remaining 50% of individuals in all these environments with an accuracy of 0.62. By adding observations in a reduced number of environments for the individuals to be predicted, while decreasing the number of phenotyped individuals across all environments, the prediction accuracy reached 1.37, highlighting the importance of phenotypic data allocation. Genomic

40 reaction norms are useful for the characterization and prediction of the function of
41 genetic parameters and facilitate breeding in a climate change context.
42

Introduction

Forest trees are keystone species in forest ecosystems supporting biological diversity and providing ecosystem services (Brockerhoff *et al.*, 2017). They also produce wood, which will be a key material for meeting the challenges of the near future, thanks to its multiple uses (construction, paper, furniture, energy, chemistry) and its ability to sequester carbon for long periods of time (Ramachandran Nair *et al.*, 2009; Domke *et al.*, 2020). In this context, forest plantation has been expanding for several decades (FAO, 2010), with the aim of concentrating timber production and relieve pressure on natural forest. However, these benefits of forest plantation will require the adaptation of forest to a new, more challenging climate (Allen *et al.*, 2010; Pawson *et al.*, 2013; Payn *et al.*, 2015) One of the major levers for ensuring sustainable wood productivity for forest plantations will be the deployment of trees capable of maintaining high growth rates even in extreme environments. To meet this goal, the integration of phenotypic plasticity, which is defined as the ability of an individual to produce different phenotypes in different environmental conditions (Bradshaw, 1965), is becoming a major issue in forest tree breeding programs (Ray *et al.*, 2022). An individual is considered here as a unique genetic combination found in a single tree, or in several vegetative copies genetically identical. The challenges posed by climate change faced limited scope of traditional genetic analyses of forest trees focusing principally on phenotypic plasticity between experimental sites (Baltunis *et al.*, 2010; Correia *et al.*, 2010; Shalizi and Isik, 2019). Although these studies

65 highlight the existence of genotype x environment (GxE) interactions for conifer
66 trees, i.e. differential variations in plasticity between individuals, they often
67 consider a limited number of environments, selected so as to avoid high mortality
68 rates. They are, therefore, not designed to be representative of the full range of
69 environments of relevance in a context of rapid climate change. The cost and
70 difficulty of exposing the same individuals to different environmental conditions,
71 particularly for species difficult to propagate vegetatively, are major obstacles to
72 the systematic evaluation of across-site plasticity in the context of tree breeding.

73 Phenotypic plasticity can be effectively modeled by reactions norms if repeated
74 measurements across ages or clones are available, together with a relevant
75 descriptor of the environment in which the phenotype was expressed (Schlichting
76 and Pigliucci, 1998; Sanchez *et al.*, 2013). A reaction norm is a representation of
77 phenotypic values as a function of an environmental gradient. Various methods for
78 constructing reaction norms have been developed, but the random regression
79 model described by (Kirkpatrick and Heckman, 1989) is particularly relevant in
80 breeding contexts. Through the integration of genetic data, this model can
81 continuously estimate genetic parameters and breeding values according to the
82 gradient. The gradient most frequently chosen is time (age), and this approach is
83 frequently used in animal breeding (Jamrozik *et al.*, 1997; Schaeffer, 2004; Boligon
84 *et al.*, 2012) and more rarely in plant breeding contexts (Sun *et al.*, 2017; Campbell
85 *et al.*, 2018) including tree breeding (Apiolaza and Garrick, 2001; Wang *et al.*, 2009).
86 However, reaction norms can also be modelled along an environmental gradient
87 (Ravagnolo *et al.*, 2000, Zumbach *et al.*, 2008, Sanchez *et al.*, 2009). In forest

88 breeding, the more recent modelling of this type of reaction norm appears to be a
89 way to meet the challenges of rapid climate change in tree breeding (Marchal *et*
90 *al.*, 2019; Alves *et al.*, 2020).

91 Selection objectives for forest tree breeding have focused mainly on the final
92 volume of the tree trunk. Historical selection criteria evaluate the size of trees at
93 an advanced age (Mullin *et al.*, 2011; Pâques, 2013). . The continuous growth of
94 trees and their reactions to the different environments encountered over the years
95 are thus summarized by a very integrative measurement. It is not therefore possible
96 to trace back and identify the environmental factors contributing to the final
97 phenotype, as environment can be considered only in a global manner over the
98 whole period. However, yearly growth increments can be correlated with well-
99 characterized environments (Martinez-Meier *et al.*, 2008; Zas *et al.*, 2020). This can
100 be achieved with the use of wood ring series, which define the annual radial growth
101 of each individual in temperate climates. Indeed, the cambial activity of trees
102 depends strongly on environmental conditions, particularly temperature and water
103 availability (Schweingruber, 2007). The variability of annual ring width and wood
104 density characterizes the plastic response of trees to changing environmental
105 conditions. It has been shown to have genetic determinism (Sánchez-Vargas *et al.*,
106 2007; Dalla-Salda *et al.*, 2009) and could be used as a proxy for the potential
107 reaction of trees to changes in environmental conditions. The analysis of these
108 repeated phenotypes therefore provides an ideal longitudinal dataset for studying
109 phenotypic plasticity at individual level (Marchal *et al.*, 2019). Such analyses can be
110 explanatory in nature, seeking to identify the optimal combination of

111 environmental factors making a significant contribution to annual growth, but they
112 can also be predictive, with the development of functional models for inferring
113 growth in environments where individuals have not been observed.

114 The integration of molecular markers into genetic evaluations provides not only
115 more accurate estimates of genetic parameters, but also opportunities to
116 implement genomic selection (GS) approaches (R2D2 Consortium *et al.*, 2021). In
117 forest trees, such approaches pave the way for the early selection of important
118 traits, such as wood traits, that would otherwise be measured only after many years
119 of cumulative growth. GS is also particularly valuable in tree breeding, as it allows
120 the integration of traits that are costly and complex to measure (Grattapaglia and
121 Resende, 2011). In many species, the gains provided by the use of genomic data
122 have tended to eclipse the interest in longitudinal data (Oliveira *et al.*, 2019).
123 However, these two approaches are not antagonistic and their beneficial effects
124 can be combined (Rutkoski *et al.*, 2016; Sun *et al.*, 2017). Genomic reaction norms
125 based on environmental measurements are rarely used (Ly *et al.*, 2018), but are
126 potentially of great value in this context, as they allow prediction of growth in as
127 yet environments where individuals have not been observed, thus decreasing the
128 complex and costly evaluation procedures associated with experimentation and
129 phenotyping under different environmental conditions.

130 We propose here an integration of environmental information into genetic
131 evaluations, using reaction norms in the context of forest tree breeding. A random
132 regression model based on annual ring growth data for maritime pine (*Pinus*

133 *pinaster* Ait.) and including genomic data was used to fit individual-level reaction
134 norms. The genetic components of these norms were described and the
135 implications of their use in the context of breeding were further investigated with
136 respect to a classical analysis targeting final radial growth. Finally, we investigated
137 the model's ability to predict the growth of individuals in environments where they
138 have not been observed, considering realistic phenotyping conditions for the
139 maritime pine breeding program in a GS context. To our knowledge, this is the first
140 study in a tree breeding context to use a random regression model to combine
141 environmental gradient and genomic information.

Materials and Methods

Plant material

A maritime pine trial was established at two sites in 1997: Site 1 (Cestas, France: Lat 44.74, Lng -0.68) and Site 2 (Escource, France: Lat 44.16, Lng -1.03). Soil characterization revealed lower soil fertility (+16.8 g organic matter/kg of soil) and a deeper water table (mean difference of +6 m) at Site2 than at Site1. Climatic measurements showed that there was more rainfall at Site 2 (mean of +15% for total annual rainfall), whereas temperatures were similar at the two sites (supplementary Table S1). A total of 192 half-sib families obtained from crosses between identified seed parents and two pollen mixtures of identified donors were studied here. 171 families were planted on both sites with 35 individuals per family in a complete block design with single-tree plots (1,250 trees/ha). 21 families were planted on Site2 only, with the same design. Each site also includes 5 checklots composed of individuals from improved and unimproved reference varieties. Thinning operations were performed at both sites in 2012 and exclusively at Site 1 in 2017, when the trees were 16 and 21 years old, respectively. A subsample (POP) of 25 half-sib families, with 13 individuals per family and per site, was selected as representative of the variability of growth (total of 650 individuals). In the absence of cloning in this maritime pine experimental context, the notions of “individual”, “tree” and even “genotype” are considered equivalent in our study.

Genetic characterization of POP

Genomic DNA was extracted from needles collected from POP, to which we added 186 randomly selected duplicates for repeatability estimates. The concentration and quality of DNA for each sample were determined with a NanoDrop spectrophotometer (NanoDrop Technologies, Wilmington, DE, USA). Genotyping was performed by Thermo Fisher Scientific (Thermo Fisher Scientific, Santa Clara, CA, USA) with the 4TREE Axiom single nucleotide polymorphism (SNP) multi-species array (Guilbaud *et al.*, 2020). Of the 50,000 SNPs on this array, 13,407 have been designed for maritime pine and are considered polymorphic for this species. The preliminary filters recommended by Thermo Fisher Scientific were applied to the genotyping results, at the sample (DishQC ≥ 0.4, CallRate ≥ 90) and SNP (CallRate ≥ 95, fld-cutoff ≥ 3.2, het-so-cutoff: ≥ -0.1) levels. In addition, sequential filtering was applied, with the removal, in the following order, of SNPs with less than 85% repeatability, SNPs with more than 5% Mendelian segregation errors and SNPs with a minor allele frequency (MAF) below 1%. A genomic relationship matrix (G) was calculated with the VanRaden formula (VanRaden, 2008) using the AGHmatrix package (Amadeu *et al.*, 2016) in R 4.2.2 environment (R Core Team, 2022):

$$G = \frac{(M - P)(M - P)'}{2\Sigma\, p_i(1 - p_i)} \quad (1)$$

where the M matrix (n: number of individuals x m: number of markers) contains marker information coded as -1 for one of the homozygotes, 0 for heterozygotes and 1 for the other homozygotes; and the P matrix (n x p) contains allele

frequencies expressed as $2(p_i - 0.5)$, where p_i is the frequency of the second allele at locus i for all individuals.

In addition, pedigree recovery was performed for each tree from POP, with a subset of 161 SNPs used to infer the identities of the parents (25 seed parents and 85 pollen parents) and grandparents (69 initial progenitors from the base population of the breeding program) (supplementary Method. S1). The most complete version of the pedigree was used to compute an additive relationship matrix A for further analyses.

Phenotypic data

Circumference measurements were performed at breast height (~1.30m from the ground) on all the trees in the trial in 2004, 2008, 2012 and 2018, at the ages of 8, 12, 16 and 22 years, respectively. In addition, cores were removed from the trees of POP in December 2019, at breast height, along the same north-south direction for each tree. These cores were cut into 2-mm-thick radial strips for X-ray analysis (Polge, 1966) to obtain wood density profiles (Fig. 1). The limits between the different rings were identified with Windendro software (Guay *et al.*, 1992) and validated by visual examination. The area of ring y (RA_{raw_y}) was calculated at individual level as follows:

$$RA_{raw_y} = \pi \left(L + l_y\right)^2 - \pi L^2 \quad (2)$$

where L is the sum of the ring widths from the pith to ring y (ring y excluded) and l_y is the width of ring y. RA_{raw} values are a good proxy for biomass produced each

year independently of tree age, in contrast to ring widths which tend to decrease progressively over the years due to radial growth of the tree.

We chose to study the 2005-2019 period (15 successive years) here because rings for this period were available for at least 99% of POP and this period excludes the juvenile phase of the trees (supplementary Table S2 and Fig. S1). Using the circumference measurements, RA_{raw} values were spatially corrected for each site with spline functions (via the BreedR R package; Muñoz and Sanchez, 2020; see supplementary Method. S2) and named RA (adjusted ring area). A complete phenotyping series for an individual is thus composed of 15 RA values.

Characterization of the environment during ring growth

The environmental conditions associated to each ring were characterized with two classes of environmental indices, which depend on both year and site variables. The first class focused on a purely climatic description, with two versions (DM and DM') of the de Martonne aridity index (de Martonne, 1926), whereas the second provided a finer description of the environmental conditions with two indices (GP and GP'), extracted from an ecophysiological model combining climatic, silvicultural and soil data (Moreaux *et al.*, 2020).

The de Martonne aridity index was calculated for each ring formed in year y at site z with:

$$DM_{y,z} = \frac{1}{8}\sum_{i=3}^{10}\frac{12P_{i,z}}{T_{i,z}+10} \quad (3)$$

where $P_{i,z}$ is the amount of precipitation (in mm) and $T_{i,z}$ is the mean air temperature (in °C), for month i in site z. Only the 8 months from March ($i = 3$) to

October ($i = 10$) were included here as we considered, as a first approximation, that climatic conditions outside the growth period of maritime pine has no impact on annual RA. In addition, we considered a modified version of the de Martonne index (DM') based on a 30-day sliding window average (instead of calendar months) and considering the impact of the climate of year $(y - 1)$ on environmental conditions in year y (inspired by Botzan *et al.*, 1998, supplementary Method. S3A). The environmental indices of the second class derived from the ecophysiological model GO+ 3.0 (Moreaux *et al.*, 2020) based on climatic data, silvicultural parameters, soil water properties, soil fertility and reference values for maritime pine growing in the Landes massif (supplementary Method. S3B). The growth potential index (GP) was calculated for each ring, based on mean trunk water potential and temperature estimated daily by the GO+ model (supplementary Method. S3C). Similarly, to the de Martonne aridity indices, a second index GP' was used to consider a sliding window of 10 days over the course of a year and to take into account the impact of previous year.

Genetic analysis of radial growth with a random regression model (RRM)

Unlike a standard analysis of radial tree growth based on final circumference measurements (supplementary Method. S4), we proposed here to model individual RA series for POP as a function of the environmental gradient, using an RRM implemented in Wombat software (Meyer, 2007). The environmental gradients associated with the four indices previously described were modeled independently

248 according to the RRM formulation. Regardless of the environmental index used, the
249 joint analysis of the two sites and year series provided an overall environmental
250 gradient of 30 levels (15 environmental levels per site). Legendre polynomials were
251 used as the base functions (Kirkpatrick *et al.*, 1990) for the following RRM (Mrode
252 and Thompson, 2005):

253 $$RA_{ijs} = \sum_{k=0}^{k_m} \Phi_{\mathrm{ijk}}\, \mathrm{m}_{\mathrm{sk}} + \sum_{k=0}^{k_\alpha} \Phi_{\mathrm{ijk}}\, \alpha_{ik} + \sum_{k=0}^{k_p} \Phi_{\mathrm{ijk}}\, \mathrm{p}_{\mathrm{ik}} + e_{ijs} \qquad (4)$$

254

255 where RA_{ijs} is the ring area of individual i for environmental level j at site s; m_{sk}
256 is the k^{th} fixed regression coefficient used to model the average trajectory at site s;
257 α_{ik} and p_{ki} are the k^{th} random regression coefficients for the genetic additive and
258 permanent environmental effects, respectively, of individual i, the latter effect
259 representing the similarity between repeated records for the same individual of
260 environmental and non-additive genetic origin; Φ_{ijk} is the k^{th} Legendre polynomial
261 for the RA of individual i at environmental level j; k_m, k_α, k_p are the order of
262 polynomials for mean trajectory, genetic additive and permanent environmental
263 effects, respectively; and r_{ijs} is a random residual. The goodness-of-fit of the
264 models for the different orders of the polynomials used was assessed by comparing
265 Aikaike information criterion (AIC) and Bayesian information criterion (BIC)
266 (supplementary Fig. S2). According to these criteria, the order 2 and order 3 models
267 appeared to be the most relevant models for the environmental indices and
268 relationship matrices considered in this study. Order 2 models have been preferred

since they allows a drastic reduction in computational demand with no loss or marginal loss of goodness-of-fit compared to order 3 models. By setting $k_m = k_\alpha = k_p = 2$, we fitted a baseline, a linear and a quadratic regression on RA.

The equivalent matrix notation for this model is (Mrode and Thompson, 2005):

$$y = Xb + Zu + Qpe + e \quad (6)$$

where y is the vector of RA over the environmental levels; b is the vector of solutions for site fixed effect; u and pe are the vectors of the individual genetic additive and permanent environmental random regression coefficients, respectively; e denotes the residuals. X, Z and Q are the corresponding incidence matrices. For genomic-based RRM, it is assumed that $u \sim N(0, G \otimes \Omega)$, $pe \sim N(0, I \otimes \mathrm{P})$, and $e \sim N(0, I \otimes \mathrm{D})$, where $\otimes$ denotes the Kronecker product, G the relationship matrix described above, Ω and P the covariance matrices for the RR coefficients for the genetic additive and permanent environmental effects, respectively, and D is a diagonal matrix of heterogeneous residuals for each environmental level. For pedigree-based RRM, G is replaced by A.

With a second-order model ($k_m = k_\alpha = k_p = 2$), the RRM estimates three genetic coefficients per individual. From these, individual GEBV were then obtained at all environmental levels as a trajectory, following the formulation of (Mrode and Thompson, 2005). GEBV estimated with an RRM integrating all available phenotypic data and solved at each environmental level are denoted $\mathrm{GEBV}_{\mathrm{ref}}$.

Genomic selection

Cross-validation (CV) scenarios

The prediction accuracy of the RRM was assessed over two CV scenarios (Fig. 2). First, the reference scenario, denoted **CV-A**, where the training set (T_{set}) included the complete phenotyping series for 50% of the individuals (randomly selected within sites and families), whilst the remaining 50% of individuals constituting the validation set (V_{set}). Second, the CV-B scenario explored the possibility of retaining the same amount of phenotypic information as for the CV-A (i.e. 50% of total phenotypic data) but distributed differently over the individuals. Scenario **CV-B** mimicked the use of a high-throughput phenotyping tool for quick estimation of the last five RA which, in a context of global warming, would typically correspond to unfavorable years. The T_{set} for **CV-B** included complete phenotypic series (i.e. 15 phenotypic records per individual) for 25% of individuals and only five phenotypic records for the remaining individuals (75% of individuals). For each site, we kept the same five environments for each repetition of the CV scenario. These 5 environments were chosen to represent the most unfavorable half of the gradient. The Kennard-Stone algorithm (Kennard and Stone, 1969) was applied via the prospectr R package (Stevens and Ramirez-Lopez, 2022) to maximize the Euclidean distances between the GP' values and thus select 5 representative environments from the 8 most unfavorable environments at each site.

The prediction accuracy (i.e. the correlation between the true and predicted breeding values) of the RRM was estimated for each environmental level as the

Pearson correlation coefficient between predicted ($GEBV_{pred}$) and observed RA in V_{set} divided by the square root of heritability. The overall prediction accuracy was then obtained by averaging the prediction accuracies of each environment. For each CV scenario, 10 independent repetitions of this process were performed. Such performance estimator was used as a criterion for assessing modeling quality (Ly *et al.*, 2018; Arnal *et al.*, 2019; Momen *et al.*, 2019).

Genetic gains

The prediction accuracy of the RRM for genetic gains in our reference scenario CV-A was assessed over each of the environmental levels. The assessment consisted of calculating the differences in genetic gain between a selection based on $GEBV_{pred}$ obtained in V_{set} and the corresponding maximum that would have been obtained with the same selection intensity based on $GEBV_{ref}$. For this, at each environmental level, the top 5% of individuals selected according to $GEBV_{pred}$ were identified and their corresponding $GEBV_{ref}$ (obtained with all the phenotypic information) used to calculate the true genetic gain (GG_{true}) as the $GEBV_{ref}$ average of the selected individuals. This amount was compared for the corresponding environmental level to the maximum gain (GG_{max}), which was calculated as the $GEBV_{ref}$ average of the top 5%. Finally, GG_{true} and GG_{max} were centered and reduced to ensure comparability between environmental levels. Any difference between GG_{true} and GG_{max} would indicate a decrease in the correlation between $GEBV_{pred}$ and $GEBV_{ref}$ for the selected percentage.

Results

Size and genetic characterization of POP

After phenotype curation (9 wood-density profiles were excluded as they were not readable enough to allow ring limits to be positioned with confidence) and genotyping quality control (13 individuals excluded), POP was finally composed of 628 trees (303 from Site 1 and 325 from Site 2).

Pedigree recovery on POP validated 93% of the pedigree seed parents (monoicous individuals acting as mothers) and allowed the correction of 5%. The remaining 2% of the pedigree seed parents was classified as unknown, as no candidate parent could be validated. Pollen parents (acting as fathers) were successfully recovered for 65% of the individuals. Note that the original design of the study was based on crosses with a mixture of pollen donors, resulting in the fathers initially being unknown in the pedigree. Finally, based on the curated pedigree, a status number (N_s; Lindgren *et al.*, 1996) of 21 was obtained for POP, suggesting a high level of relatedness between the families studied.

The genotyping of POP resulted in the characterization of the 628 individuals over 3,832 SNPs, with a repeatability of 97% and a total missing data rate of 1%. Additive genomic relationship coefficients (g_{xy}) estimated in G were consistent with the pedigree-based additive relationship coefficients (a_{xy}) calculated in A (Fig. 3). The a_{xy} values were discrete, whereas the g_{xy} values were normally distributed for each level of relatedness. Note that, for most pedigree-based additive coefficient levels, the normal distribution has a long upward-sloping tail (revealing some rare

cases of unrecorded relatedness), and a mean slightly below the theoretical value, the latter being represented by the gray line in Fig. 3. This shift is expected insofar as the standardization of G matrix with the observed allele frequencies sets its average to 0.

Quality of model fit

The prediction accuracy (estimated with CV-A) was used as a criterion for assessing the quality of RRM (Fig. 4). Mean prediction accuracies were moderate to high, with correlation coefficients ranging from 0.19 to 0.25. Prediction accuracy was slightly better (+0.04 better, on average) for genomic-based RRM than for pedigree-based RRM, except for RRM based on the DM environmental index (equivalent mean prediction accuracy of 0.21). The best prediction accuracies were obtained for genomic-based RRM with the DM' (0.24) and GP' (0.25) indices. The optimization of environmental indices improved slightly RRM prediction accuracy by 16% and 3% relative to the initial DM and GP indices, respectively. Finally, the genomic-based RRM using the GP' index was selected for the analyses described below, due to its best prediction accuracy (0.25) for GS. Detailed prediction accuracies by environment for this model are presented in the supplementary Fig. S3.

Narrow-sense heritability estimated for this model varied between 0.12 and 0.24 over the environmental gradient (supplementary Fig. S5). Despite the high level of variation between similar environmental levels, heritability was significantly higher for the most favorable environmental levels.

Individual reactions norms estimated by genomic-based RRM

Reordering longitudinal data by the annual environmental index, which characterizes the conditions of ring formation, instead of the ordinal year greatly modified the shape of the mean RA curve in a more easily interpretable way (Fig. 5). When expressed as a function of the environmental index GP', RA increases significantly. The lowest GP' values are associated with the most unfavorable environmental conditions for growth, whereas the highest values are associated with the most favorable conditions for growth. This pattern suggests plasticity at the population level, but hides individual behaviors, which may deviate from this central trajectory.

Random individual deviations from the mean trajectories due to additive genetic effects are represented in Fig. 6 and were solved over the environmental gradient of GP' ($GEBV_{ref}$). For most individuals, $GEBV_{ref}$ showed a dependence on GP', highlighting the existence of plasticity for RA. These different behaviors can be characterized simply by the slope of the trajectories, depicted in different colors (Fig. 6). A majority of individual reaction norms were were characterized by shallow slopes and mean $GEBV_{ref}$ close to 0. This does not mean that the phenotypic trajectory of these individuals is flat. Instead, it indicates that they have trajectories indistinguishable from the mean trajectory and due to its additive genetic origin, they would give only very limited extra plasticity to the offspring, unlike individuals whose trajectories are significantly further from 0. The highest and lowest mean $GEBV_{ref}$ were those obtained for individuals whose trajectory is colored dark blue

and dark red, respectively. These individuals also display reaction norms with the strongest positive and negative slopes (for dark blue trajectories anddark red trajectories, respectively), leading to a greater range of variation in individual genetic values in favorable than in unfavorable environmental levels. The average $GEBV_{ref}$ for each individual is, thus, strongly correlated with the regression coefficients describing the slope of its trajectory (+0.52 and +0.95 with quadratic and linear regression coefficients, respectively). There appear to be few intersections between reaction norms, corresponding to changes in individual ranks across environmental levels, over most of the environmental gradient. This is confirmed by strong genetic correlations (>0.90) between environmental levels (supplementary Fig. S4). However, large overlaps occur in the part of the gradient corresponding to unfavorable environmental levels (Fig. 6). This results in lower genetic correlations (between 0.83 and 0.90) between the two most unfavorable environmental levels (GP'=52 and GP'=53) and more favorable environmental levels (when GP'>65). These lower values point out variations in how certain individuals behave at these unfavorable environmental levels, which affects their ranking.

Genomic selection scenarios and cross-validation

Genetic gain over the environmental gradient

The overall prediction accuracy of the genomic-based RRM (using the GP' environmental index) estimated with the CV-A scenario was 0.62 (Fig. 4). Breeding

efficiency, based on predicted values, was assessed by calculating genetic gains for different environmental levels (Fig. 7). GG_{max} increased until the environmental value of 62, above which it reached a plateau with maximum value of 2.35. The difference between GG_{max} and GG_{true} was minimal (+0.64) for GP' environmental level 62, increasing towards the two extreme environmental levels. Indeed, this difference reached +0.73 and +0.72 respectively for the most unfavorable environmental level 53 and for the most favorable environmental level 82. The relatively moderate prediction accuracy of the RRM (0.62) necessarily led to a significant loss of genetic gain (no overlap between GG_{max} and GG_{true} boxplots). Nevertheless, depending on the environmental level, GG_{true} accounted for 68% to 73% of GG_{max}. GG_{true} was always significantly different from 0 ($p - value_{t-tes} < 0.001$), indicating a certain efficiency of selection based on predicted values, even in the most extreme environmental levels.

Prediction accuracy over the CV scenarios

We considered an alternative cross-validation scenario (CV-B) (Fig. 2), to improve selection efficiency while preserving phenotyping effort with respect to CV-A. As in CV-A, 50% of the phenotypic data were used to constitute the T_{set} of the CV-B. The key difference between the two is due to a better distribution of phenotypic effort, both between individuals and between environments, in CV-B. This alternative distribution had a considerable impact on improving the prediction accuracy of the RRM, which increased from 0.62 for the CV-A to 1.37 for the CV-B (Fig. 8), with no increase in phenotyping effort. It should be noted that the CV-A scenario is a major challenge for RRM, as it imposes the prediction of entire trajectories for half of the

population. This challenge is relaxed in CV-B by including at least partial information for all individuals.

Discussion

Deciding which genetic material should be planted now to form the forests of tomorrow is becoming increasingly challenging due to the rapidity of climate change (Thomas *et al.*, 2004; Wiens, 2016). Using longitudinal tree-ring data and parallel environmental descriptors, we have successfully modeled genomic individual reaction norms based on random regression. This first example for forest trees provided consistent results for use in the maritime pine breeding program, but may inspire other programs in perennial species.

Reaction norms in forest trees

Growth measurements at advanced age are generally used for the calculation of breeding values. Such measurements constitute highly integrative phenotypes that can be associated only with a global environmental site index. Using sites with contrasting indices has been a classic strategy to establish comparative trials for genetic x environment evaluation. In this sense, our two sites present strong contrast in terms of fertility and water table depth at the scale of the Landes massif, but even with their differences they are still part of the same breeding area (Jolivet *et al.*, 2007). Wood cores give us access to phenotypic inter-annual variation and can be used to generate longitudinal annual growth data that can be associated

with annual environmental variation. Our results showed indeed that the environmental variation between years was much greater than the one between sites (Fig. 5). Indeed Cir22 was associated with a mean environmental index GP' of 68.2 for site 1 and 72.1 for site 2, whereas analysis based on ring measurements covered a larger index range (GP' from 52.6 to 81.9). This much greater annual variation provides an opportunity to infer plasticity at individual level over a large environmental gradient.

In addition to longitudinal data collection, which can be operationally costly, there are other challenges that arise with these data. One is autocorrelation between repeated measurements on the same individual in a time series. Another, not least, is ontogenetic differences between phases of phenotype expression (Sanchez *et al.*, 2013). Finally, a third challenge is the choice of a relevant environmental descriptor. Although we have not shown it for simplicity, we have performed a preliminary RRM for RA with a one-year lag in the climatic index in order to match RA of year *n* with the environmental index of year *n - 1*, and its results pointed to an absence of autocorrelated effect. As for the ontogeny challenge, we have ignored in our longitudinal data series the initial segments corresponding to the juvenile phase, keeping only the remaining adult phase for which the RA trend was generally flat, despite strong inter-annual oscillations (Fig. 5A).

The third challenge is probably the most difficult to address, the choice of a relevant environmental index (Li *et al.*, 2017). This study was not designed to identify precisely the environmental factors most relevant to tree growth, but we defined

485 two classes of biologically meaningful environmental indices that integrate the key
486 components of temperature and water (Begum *et al.*, 2013; Rathgeber *et al.*, 2016).
487 Both of them depend on the year and the site in which the ring was formed. The
488 first class (aridity indices) is easy to obtain, since it only considers the climatic data
489 (temperature and precipitation over the growing period) of the site and the year
490 associated with to the rings under study. On the other hand, the second class
491 (growth potential indices) requires more complex modeling, including for example
492 the characterization of the daily water status of the trunk. A major difference
493 between the two types of indices is the insensitivity of the former to the intra-
494 annual distribution of precipitation and temperatures. Thus, similar annual aridity
495 values (DM or DM') may reflect different climatic realities over the course of the
496 growing season, with temperatures and/or precipitation occurring at different
497 periods and leading to differences in growth. Conversely, by considering the daily
498 environmental status and tree physiology, the growth potential indices (GP and
499 GP') allowed a more detailed consideration of within-year environmental variation.

500 Finally, the prediction accuracy obtained with DM, DM', GP, GP' (Fig. 4) confirms
501 the relevance of the proposed environmental indices, but also suggest that they
502 only partially capture the environmental factors influencing radial growth and the
503 differences between individuals' reactions. More specifically, the variability due to
504 site is not fully described by the index, given the remaining high significance value
505 of the corresponding fixed effect in RRM (Fig. 5B).

Modelling reaction norms with RRM

Unlike univariate single-point analyses, which are easy to implement but do not integrate longitudinal phenotypic information, or multi-trait models, which can integrate it but are computationally demanding, RRM provides genetic estimates over the chosen continuous environmental gradient with reduced parametrization (Sun *et al.*, 2017). The continuous trajectory of GEBV predicted by the RRM allows a position to be considered at any environmental level within the range defined by the two most extreme environments, whether it has actually been observed or not. The RRM can model highly complex curves using orthogonal base functions such as Legendre polynomials, which are widely used and described in the context of breeding (Schaeffer, 2004; Campbell *et al.*, 2018; Marchal *et al.*, 2019). Despite their great flexibility and computational advantages, Legendre polynomials may present numerical problems (Runge's phenomenon) at the extremities for high-order fits (de Boor, 1978; Meyer and Kirkpatrick, 2005). In this study, the adjustment at the extremities of the environmental gradient was particularly important as the unfavorable extreme conditions are likely to increase in frequency in the future (Coumou and Rahmstorf, 2012; Spinoni *et al.*, 2018). The use of low-order polynomials to model RA trajectories overcame this problem. The consistency and quality of the norms fitted with Legendre polynomials were verified by a comparison with norms fitted with B-spline functions, which are considered a more robust alternative to high-order polynomials in terms of extremum fitting, although less advantageous computationally (de Boor, 1978; Meyer and Kirkpatrick, 2005) (Kendall correlations between $GEBV_{ref}$ estimated with

529 Legendre polynomials and those estimated with B-splines yielding coefficients of
530 up to 0.95 over the entire gradient for the final RRM).

531 Exploration of individual genetic trajectories

532 Random individual trajectories (Fig. 6) highlight the existence of plasticity for
533 genetic values that can be targeted by breeders. It is not easy to discriminate
534 between individual reaction norms that follow a trajectory close to the population
535 average, given their high frequency, the fact that they present shallow slopes and
536 mean $GEBV_{ref}$ close to 0. However, individuals with potentially good growth along
537 the entire gradient are much easier to discriminate from the rest, for which the
538 proposed clustering allows simple and efficient visualization (cluster E), useful for
539 selection purposes.

540 The distribution of individual GEBV varied between environmental levels, and those
541 more favorable levels enhanced the expression of differences between trajectories
542 relative to less favorable levels, which has already been observed in other biological
543 models (Arnold *et al.*, 2019). Individual ranking was globally preserved over the
544 trajectories for most of the gradient (van Eeuwijk *et al.*, 2016). This trend was
545 confirmed by strong genetic correlations (supplementary Fig. S4) between the
546 environmental levels. However, these genetic correlations were weaker with
547 unfavorable environments (environmental index below 65), in agreement with the
548 reranking of individuals observed for the individual trajectories at the most
549 unfavorable end (Fig. 6). This precise and localized GxE interaction in our gradient,
550 only possible thanks to the use of the RRM, should not be considered marginal or

potentially negligible considering that it affects only one segment of the gradient. In fact, climate projections (supplementary Fig. S6) suggest that such unfavorable environments are likely to become much more common in the future. Even if the expected global level of aridity in 2075 remains close to current levels, according to our de Martonne calculation, aridity in 2100 will be much stronger, with a higher frequency of extreme events as predicted by other studies (Sillmann and Roeckner, 2008; Lehner *et al.*, 2017). Our 15-year study period was already affected by a high global level of aridity and included extreme annual climates that may become frequent in the future. The environmental gradient used for the inference of reaction norms is therefore particularly relevant for identifying individuals with better potential for growth in the unfavorable years to come.

When GxE interactions must be taken into account in selection decisions, a robust strategy would involve prioritizing the best adapted individuals across the entire environmental gradient (Li *et al.*, 2017), focusing on the notion of persistence. The definition of persistence may vary according to species and breeding aims (Gengler, 1996; Rocha *et al.*, 2018), but it is generally defined as the capacity of a species to maintain a stable or high level of growth or production over time or in the face of different environmental conditions. For reactions norms, several ways of evaluating persistence and integrating the slope of trajectories in an operational breeding context have been proposed. For example, for feed conversion ratio in large white pigs, (Huynh-Tran *et al.*, 2017) suggested combining the EBV estimated by the RRM with the coefficients of eigenvectors estimated from the eigenvalue decomposition of the covariance matrix of additive genetic effects. In their study, two summarized

574 breeding values for each individual were sufficient to describe most of the variation
575 in terms of mean genetic values (first dimension) and the slopes of EBV trajectories
576 (second dimension), and could be used directly in selection. In another example in
577 goat lactation, (Arnal *et al.*, 2019) considered "the cumulative deviation in genetic
578 contribution to yield relative to an average animal having the same (initial) yield"
579 for the calculation of persistence-related EBV. Finally, (Peixoto *et al.*, 2020)
580 suggested the ranking of cotton genotypes on the basis of area under the reaction
581 norm, the genotype with the highest norm being the most persistent. Another
582 interesting approach would involve calculating the final GEBV for each individual as
583 the mean of the GEBV for each environmental level weighted by the probability of
584 occurrence of the environmental level in the future. Such a strategy would make
585 use of the GxE interaction to maximize genetic gain for individuals performing in
586 environmental conditions close to those predicted for the near future, while
587 ensuring a certain level of resilience to environmental variation. Any of these
588 proposals could be applied to our data. A possible advantage of the latter strategy
589 could be to take more explicit account of future climate predictions, provided that
590 they have some control over uncertainty.

591 ## Reaction norm in a GS context

592 The use of genomic reaction norms to predict the growth of individuals in
593 environments where they have not been observed is a good example of the
594 potential benefits of GS approaches for traits that are complex to evaluate. Wood
595 density profiles provide highly informative longitudinal data on tree growth over

596 the years, but its acquisition via the coring process remains costly and time-
597 consuming at breeding-program scale. This limitation has motivated one of our
598 alternative cross-validation scenarios (CV-B), with a more homogeneous
599 distribution of phenotypic effort, resulting in a training population involving all
600 individuals, 25% of which contribute full time series and the remaining 75% only
601 partial 5-year series. Indeed, relative to our baseline scenario (CV-A), which aimed
602 to predict the full trajectories of 50% of individuals, the CV-B scenario achieved a
603 much higher level of prediction accuracy (1.37), demonstrating that the allocation
604 of phenotyping effort to constitute the training population is a key optimization to
605 consider. The scenario CV-B would reflect the use of a high-throughput
606 phenotyping tool usable on a large number of individuals at the cost of a smaller
607 number of rings scanned per tree, which is basically what a resistograph does
608 (Bouffier *et al.*, 2008). Resistograph measures the resistance of the wood to
609 penetration with a needle and can estimate RA efficiently for the rings closest to
610 the bark, i.e. the last five rings formed (personal communication). These
611 measurements provide only partial information about plasticity, but when applied
612 to the whole population, they have the advantage of providing information
613 complementary to that obtained by coring. Overall, less phenotyping effort is
614 required, but the benefits are substantial.

615 The genetic component of reaction norms, the one of greatest interest to breeders,
616 was estimated by integrating pedigree or genomic information in the RRM.
617 Genomic-based RRM had a significantly better prediction accuracy (with the GP'
618 index) than pedigree-based RRM, suggesting that refining the coefficients of

relationships between individuals through their molecular characterization with SNPs results in the generation of more suitable models (Gamal El-Dien *et al.*, 2016; Bouvet *et al.*, 2016). The pedigree information tended towards a systematic overestimation of pairing coefficients relative to the genomic information (Fig. 3). However, some rare pairs of individuals appeared to be much more related on the basis of genomics than on the basis of pedigree, suggesting that, in some cases, the pedigree may be incomplete, or may contain errors, despite the correction and recovery steps (Tan *et al.*, 2017; Li *et al.*, 2019). The use of genomic data for genomic evaluation is often proposed for forest trees (Grattapaglia and Resende, 2011; Lebedev *et al.*, 2020), but first GS studies for maritime pine (Isik *et al.*, 2016; Bartholomé *et al.*, 2016) highlighted the difficulty of demonstrating a superiority of genomic models over pedigree-based models. In this study, we provide some arguments to go beyond these limitations in the application of the genomic prediction model. The RRM takes greater advantage of genomic information to predict individual trajectories than pedigree information. Indeed, in a context of intense climate change, the importance of integrating environmental information into genetic evaluation may fully justify the additional cost of genotyping (Isik, 2014).

Acknowledgments

This work was supported by the European Union's Horizon 2020 Research and Innovation Programme Project under grant agreement n°773383 (B4EST). VP was awarded a doctoral fellowship (N°2020-CK-126) from Ecole Nationale Supérieure Des Sciences Agronomiques de Bordeaux-Aquitaine, 1 cours du Général de Gaulle, CS 40201 33175 Gradignan Cedex. The authors would like to thank GIS "Groupe Pin Maritime du Futur" and INRAE - UEFP (https://doi.org/10.15454/1.5483264699193726E12) for the installation of the studied sites, the management of the sites, the help to collect data (circumference measurements) and biological material (needles and increment cores). Authors are thankful to Frederic Lagane (PHENOBOIS Platform) for the cutting and the radiography of the increment cores. Authors thank the Institute of Biosciences and BioResources – Italian National Council of Research (IBBR/CNR), especially Giovanni Giuseppe Vendramin and Sara Pinosio for performing most of DNA extraction and quality monitoring. Part of the experiments (DNA extraction, quantification and manipulation) were also performed at the PGTB (doi:10.15454/1.5572396583599417E12), with the help of Christophe Boury and Céline Lalanne. Raphaël Segura provided soil and climate characterization for the two studied sites. Authors are also thankful to Christophe Plomion for his help during the conceptualization of this study.

Author contributions

LB and LS: conceptualization, supervision and validation

VP, AB, LB and LS: methodology

VP: data curation, formal analysis, visualization, writing – original draft preparation

VP and AB: software

AB, LB and LS: writing – Review & Editing

Competing Interests

The authors declare no competing financial interests

Data Archiving

The data underlying this article are accessible via the private following link (Data INRAE):

https://entrepot.recherche.data.gouv.fr/privateurl.xhtml?token=15f2101e-ebb8-4b7c-838b-9703090cfec4

The corresponding DOI is https://doi.org/10.57745/NUTK1I (Papin, Victor; Bosc, Alexandre; Sanchez-Rodriguez, Leopoldo; Bouffier, Laurent, 2023)

The data will be made public and accessible to all once the article has been accepted.

Research Ethics Statement

Not applicable.

References

Allen CD, Macalady AK, Chenchouni H, Bachelet D, McDowell N, Vennetier M, *et al.* (2010). A global overview of drought and heat-induced tree mortality reveals emerging climate change risks for forests. *Forest Ecology and Management* **259**: 660–684.

Alves RS, de Resende MDV, Azevedo CF, Silva FF e., Rocha JR do AS de C, Nunes ACP, *et al.* (2020). Optimization of Eucalyptus breeding through random regression models allowing for reaction norms in response to environmental gradients. *Tree Genetics & Genomes* **16**: 38.

Amadeu RR, Cellon C, Olmstead JW, Garcia AAF, Resende MFR Jr, Muñoz PR (2016). AGHmatrix: R package to construct relationship matrices for autotetraploid and diploid species: a blueberry example. *The Plant Genome* **9**: 1–10.

Apiolaza LA, Garrick DJ (2001). Analysis of longitudinal data from progeny tests: some multivariate approaches. *Forest Science* **47**: 129–140.

Arnal M, Larroque H, Leclerc H, Ducrocq V, Robert-Granié C (2019). Genetic parameters for first lactation dairy traits in the Alpine and Saanen goat breeds using a random regression test-day model. *Genetics Selection Evolution* **51**: 43.

Arnold PA, Kruuk LEB, Nicotra AB (2019). How to analyse plant phenotypic plasticity in response to a changing climate. *New Phytol* **222**: 1235–1241.

Baltunis BS, Gapare WJ, Wu HX (2010). Genetic parameters and genotype by environment interaction in radiata pine for growth and wood quality traits in Australia. *Silvae Genetica* **59**: 113–124.

Bartholomé J, Van Heerwaarden J, Isik F, Boury C, Vidal M, Plomion C, *et al.* (2016). Performance of genomic prediction within and across generations in maritime pine. *BMC Genomics* **17**: 604.

Begum S, Nakaba S, Yamagishi Y, Oribe Y, Funada R (2013). Regulation of cambial activity in relation to environmental conditions: understanding the role of temperature in wood formation of trees. *Physiol Plant* **147**: 46–54.

Boligon AA, Mercadante MEZ, Lôbo RB, Baldi F, Albuquerque LG (2012). Random regression analyses using B-spline functions to model growth of Nellore cattle. *Animal* **6**: 212–220.

de Boor C (1978). *A practical guide to splines*, 2nd edn. New York: Springer Verlag.

Botzan TM, Mariño MA, Necula AI (1998). Modified de Martonne aridity index: application to the Napa Basin, California. *Physical Geography* **19**: 55–70.

Bouffier L, Charlot C, Raffin A, Rozenberg P, Kremer A (2008). Can wood density be efficiently selected at early stage in maritime pine (*Pinus pinaster* Ait.)? *Annals of Forest Science* **65**: 106–106.

Bouvet J-M, Makouanzi G, Cros D, Vigneron P (2016). Modeling additive and non-additive effects in a hybrid population using genome-wide genotyping: prediction accuracy implications. *Heredity* **116**: 146–157.

Bradshaw AD (1965). Evolutionary Significance of Phenotypic Plasticity in Plants. In: Caspari EW, Thoday JM (eds) *Advances in Genetics*, Academic Press Vol 13, pp 115–155.

Brockerhoff EG, Barbaro L, Castagneyrol B, Forrester DI, Gardiner B, González-Olabarria JR, *et al.* (2017). Forest biodiversity, ecosystem functioning and the provision of ecosystem services. *Biodiversity and Conservation* **26**: 3005–3035.

Campbell M, Walia H, Morota G (2018). Utilizing random regression models for genomic prediction of a longitudinal trait derived from high-throughput phenotyping. *Plant Direct* **2**: 1–11.

Correia I, Alía R, Yan W, David T, Aguiar A, Almeida MH (2010). Genotype × environment interactions in *Pinus pinaster* at age 10 in a multienvironment trial in Portugal: a maximum likelihood approach. *Annals of Forest Science* **67**: 612–612.

Coumou D, Rahmstorf S (2012). A decade of weather extremes. *Nature Clim Change* **2**: 491–496.

Dalla-Salda G, Martinez-Meier A, Cochard H, Rozenberg P (2009). Variation of wood density and hydraulic properties of Douglas-fir (*Pseudotsuga menziesii* (Mirb.) Franco) clones related to a heat and drought wave in France. *Forest Ecology and Management* **257**: 182–189.

Domke GM, Oswalt SN, Walters BF, Morin RS (2020). Tree planting has the potential to increase carbon sequestration capacity of forests in the United States. *Proc Natl Acad Sci U S A* **117**: 24649–24651.

van Eeuwijk FA, Bustos-Korts DV, Malosetti M (2016). What should students in plant breeding know about the statistical aspects of genotype × environment interactions? *Crop Science* **56**: 2119–2140.

FAO (2010). Global forest resources assessment: Main report. *UN Food and Agriculture Organization, Rome*.

Gamal El-Dien O, Ratcliffe B, Klápště J, Porth I, Chen C, El-Kassaby YA (2016). Implementation of the Realized Genomic Relationship Matrix to Open-Pollinated White Spruce Family Testing for Disentangling Additive from Nonadditive Genetic Effects. *G3* **6**: 743–753.

Gengler N (1996). Persistency of lactation yields: a review. *Interbull Bulletin* **12**: 87–96.

Grattapaglia D, Resende MDV (2011). Genomic selection in forest tree breeding. *Tree Genetics & Genomes* **7**: 241–255.

Guay R, Gagnon R, Morin H (1992). A new automatic and interactive tree ring measurement system based on a line scan camera. *The Forestry Chronicle* **68**: 138–141.

Guilbaud R, Biselli C, Buiteveld J, Cattivelli L, Copini P, Dowkiw A, *et al.* (2020). Development of a new tool (4TREE) for adapted genome selection in European tree species. In: *Proceedings of the Gentree Symposium*, Avignon, France, p .

Huynh-Tran VH, Gilbert H, David I (2017). Genetic structured antedependence and random regression models applied to the longitudinal feed conversion ratio in growing Large White pigs. *Journal of Animal Science* **95**: 4752–4763.

Isik F (2014). Genomic selection in forest tree breeding: the concept and an outlook to the future. *New Forests* **45**: 379–401.

Isik F, Bartholomé J, Farjat A, Chancerel E, Raffin A, Sanchez L, *et al.* (2016). Genomic selection in maritime pine. *Plant Science* **242**: 108–119.

Jamrozik J, Schaeffer LR, Dekkers JCM (1997). Genetic evaluation of dairy cattle using test day yields and random regression model. *Journal of Dairy Science* **80**: 1217–1226.

Jolivet C, Augusto L, Trichet P, Arrouays D (2007). Les sols du massif forestier des Landes de Gascogne : formation, histoire, propriétés et variabilité spatiale. *Revue forestière française* **59**: 7–30.

Kennard RW, Stone LA (1969). Computer aided design of experiments. *Technometrics* **11**: 137–148.

Kirkpatrick M, Heckman N (1989). A quantitative genetic model for growth, shape, reaction norms, and other infinite-dimensional characters. *Journal of Mathematical Biology* **27**: 429–450.

Kirkpatrick M, Lofsvold D, Bulmer M (1990). Analysis of the inheritance, selection and evolution of growth trajectories. *Genetics* **124**: 979–993.

Lebedev VG, Lebedeva TN, Chernodubov AI, Shestibratov KA (2020). Genomic selection for forest tree improvement: methods, achievements and perspectives. *Forests* **11**: 1190.

Lehner F, Coats S, Stocker TF, Pendergrass AG, Sanderson BM, Raible CC, *et al.* (2017). Projected drought risk in 1.5°C and 2°C warmer climates. *Geophysical Research Letters* **44**: 7419–7428.

Li Y, Klápště J, Telfer E, Wilcox P, Graham N, Macdonald L, *et al.* (2019). Genomic selection for non-key traits in radiata pine when the documented pedigree is corrected using DNA marker information. *BMC Genomics* **20**: 1026.

Li Y, Suontama M, Burdon RD, Dungey HS (2017). Genotype by environment interactions in forest tree breeding: review of methodology and perspectives on research and application. *Tree Genetics & Genomes* **13**: 60.

Lindgren D, Gea L, Jefferson PA (1996). Loss of genetic diversity monitored by status number. *Silvae Genetica* **45**: 52–59.

Ly D, Huet S, Gauffreteau A, Rincent R, Touzy G, Mini A, *et al.* (2018). Whole-genome prediction of reaction norms to environmental stress in bread wheat (*Triticum aestivum* L.) by genomic random regression. *Field Crops Research* **216**: 32–41.

Marchal A, Schlichting CD, Gobin R, Balandier P, Millier F, Muñoz F, *et al.* (2019). Deciphering hybrid larch reaction norms using random regression. *G3 Genes|Genomes|Genetics* **9**: 21–32.

Martinez-Meier A, Sanchez L, Pastorino M, Gallo L, Rozenberg P (2008). What is hot in tree rings? The wood density of surviving Douglas-firs to the 2003 drought and heat wave. *Forest Ecology and Management* **256**: 837–843.

de Martonne E (1926). Une nouvelle function climatologique: L'indice d'aridité. *Meteorologie* **2**: 449–459.

Meyer K (2007). WOMBAT—A tool for mixed model analyses in quantitative genetics by restricted maximum likelihood (REML). *Journal of Zhejiang University Science B* **8**: 815–821.

Meyer K, Kirkpatrick M (2005). Up hill, down dale: quantitative genetics of curvaceous traits. *Philosophical Transactions of the Royal Society B: Biological Sciences* **360**: 1443–1455.

Momen M, Campbell MT, Walia H, Morota G (2019). Predicting longitudinal traits derived from high-throughput phenomics in contrasting environments using genomic Legendre polynomials and B-splines. *G3 Genes|Genomes|Genetics* **9**: 3369–3380.

Moreaux V, Martel S, Bosc A, Picart D, Achat D, Moisy C, *et al.* (2020). Energy, water and carbon exchanges in managed forest ecosystems: description, sensitivity analysis and evaluation of the INRAE GO+ model, version 3.0. *Geoscientific Model Development* **13**: 5973–6009.

Mrode RA, Thompson R (2005). *Linear models for the prediction of animal breeding values*, 2nd ed. CABI Pub: Wallingford, UK ; Cambridge, MA.

Mullin T, Andersson Gull B, Bastien J-C, Beaulieu J, Burdon R, Dvorak W, *et al.* (2011). Economic Importance, Breeding Objectives and Achievements. In: Plomion C, Bousquet J, Kole C (eds) *Genetics, Genomics and Breeding of Conifers*, Science Publishers and CRC Press: New York, pp 40–127.

Muñoz F, Sanchez L (2020). breedR: statistical methods for forest genetic resources analysts.

Oliveira HR, Brito LF, Lourenco DAL, Silva FF, Jamrozik J, Schaeffer LR, *et al.* (2019). Invited review: Advances and applications of random regression models: from quantitative genetics to genomics. *Journal of Dairy Science* **102**: 7664–7683.

Pâques LE (Ed.) (2013). *Forest tree breeding in Europe: current state-of-the-art and perspectives*. Springer Netherlands: Dordrecht.

Pawson SM, Brin A, Brockerhoff EG, Lamb D, Payn TW, Paquette A, *et al.* (2013). Plantation forests, climate change and biodiversity. *Biodiversity and Conservation* **22**: 1203–1227.

Payn T, Carnus J-M, Freer-Smith P, Kimberley M, Kollert W, Liu S, *et al.* (2015). Changes in planted forests and future global implications. *Forest Ecology and Management* **352**: 57–67.

Peixoto MA, Coelho IF, Evangelista JSPC, Alves RS, Rocha JR do AS de C, Farias FJC, *et al.* (2020). Reaction norms-based approach applied to optimizing recommendations of cotton genotypes. *Agronomy Journal* **112**: 4613–4623.

Polge H. 1966. Établissement des courbes de variation de la densité du bois par exploration densitométrique de radiographies d'échantillons prélevés à la tarière sur des arbres vivants : applications dans les domaines Technologique et Physiologique.

R Core Team (2022). R: A Language and Environment for Statistical Computing.

R2D2 Consortium, Fugeray-Scarbel A, Bastien C, Dupont-Nivet M, Lemarié S (2021). Why and how to switch to genomic selection: lessons from plant and animal breeding experience. *Frontiers in Genetics* **12**.

Ramachandran Nair PK, Mohan Kumar B, Nair VD (2009). Agroforestry as a strategy for carbon sequestration. *Journal of Plant Nutrition and Soil Science* **172**: 10–23.

Rathgeber CBK, Cuny HE, Fonti P (2016). Biological basis of tree-ring formation: a crash course. *Frontiers in Plant Science* **7**.

Ravagnolo O, Misztal I, Hoogenboom G (2000). Genetic Component of Heat Stress in Dairy Cattle, Development of Heat Index Function. *J Dairy Sci* **83**: 2120–2125.

Ray D, Berlin M, Alia R, Sanchez L, Hynynen J, González-Martinez S, *et al.* (2022). Transformative changes in tree breeding for resilient forest restoration. *Frontiers in Forests and Global Change* **5**.

Rocha JR do AS de C, Marçal T de S, Salvador FV, da Silva AC, Machado JC, Carneiro PCS (2018). Genetic insights into elephantgrass persistence for bioenergy purpose. *PLOS ONE* **13**: 1–16.

Rutkoski J, Poland J, Mondal S, Autrique E, Pérez LG, Crossa J, *et al.* (2016). Canopy temperature and vegetation indices from high-throughput phenotyping improve accuracy of pedigree and genomic selection for grain yield in wheat. *G3 Genes|Genomes|Genetics* **6**: 2799–2808.

Sánchez JP, Misztal I, Aguilar I, Zumbach B, Rekaya R (2009). Genetic determination of the onset of heat stress on daily milk production in the US Holstein cattle. *Journal of Dairy Science* **92**: 4035–4045.

Sanchez L, Rozenberg P, Bastien C (2013). Shifting from growth to adaptive traits and competition: the prospect of improving tree responses to environmental stresses. In: *Novel Tree Breeding*, Instituto Nacional de Investigacion y Tecnologia Agraria y Alimentaria (INIA) Vol 24, p .

Sánchez-Vargas NM, Sánchez L, Rozenberg P (2007). Plastic and adaptive response to weather events: a pilot study in a maritime pine tree ring. *Can J For Res* **37**: 2090–2095.

Schaeffer LR (2004). Application of random regression models in animal breeding. *Livestock Production Science* **86**: 35–45.

Schlichting C, Pigliucci M (1998). *Phenotypic Evolution: A Reaction Norm Perspective*. Sinauer associates: Sunderland.

Schweingruber FH (2007). *Wood Structure and Environment*. Springer: Berlin.

Shalizi MN, Isik F (2019). Genetic parameter estimates and GxE interaction in a large cloned population of *Pinus taeda* L. *Tree Genetics & Genomes* **15**: 46.

Sillmann J, Roeckner E (2008). Indices for extreme events in projections of anthropogenic climate change. *Climatic Change* **86**: 83–104.

Spinoni J, Vogt JV, Naumann G, Barbosa P, Dosio A (2018). Will drought events become more frequent and severe in Europe? *International Journal of Climatology* **38**: 1718–1736.

Stevens A, Ramirez-Lopez L (2022). *An introduction to the prospectr package*.

Sun J, Rutkoski JE, Poland JA, Crossa J, Jannink J-L, Sorrells ME (2017). Multitrait, random regression, or simple repeatability model in high-throughput phenotyping data improve genomic prediction for wheat grain yield. *The Plant Genome* **10**: 1–12.

Tan B, Grattapaglia D, Martins GS, Ferreira KZ, Sundberg B, Ingvarsson PK (2017). Evaluating the accuracy of genomic prediction of growth and wood traits in two Eucalyptus species and their F1 hybrids. *BMC Plant Biol* **17**: 110.

Thomas CD, Cameron A, Green RE, Bakkenes M, Beaumont LJ, Collingham YC, *et al.* (2004). Extinction risk from climate change. *Nature* **427**: 145–148.

VanRaden PM (2008). Efficient methods to compute genomic predictions. *Journal of Dairy Science* **91**: 4414–4423.

Wang C, Andersson B, Waldmann P (2009). Genetic analysis of longitudinal height data using random regression. *Canadian Journal of Forest Research* **39**: 1939–1948.

Wiens JJ (2016). Climate-related local extinctions are already widespread among plant and animal species. *PLOS Biology* **14**: 1–18.

Zas R, Sampedro L, Solla A, Vivas M, Lombardero MJ, Alía R, *et al.* (2020). Dendroecology in common gardens: Population differentiation and plasticity in resistance, recovery and resilience to extreme drought events in *Pinus pinaster*. *Agricultural and Forest Meteorology* **291**: 108060.

Zumbach B, Misztal I, Tsuruta S, Sanchez JP, Azain M, Herring W, *et al.* (2008). Genetic components of heat stress in finishing pigs: Development of a heat load function. *Journal of Animal Science* **86**: 2082–2088.

Figures

Figure 1: From wood increment core to wood density profile. *From the bottom to the top: the wood increment core picture from one tree, its corresponding radiography, its wood density profile (black line) from pith (position: 0mm) to the bark obtained after processing. Sudden and high drops in wood density mark the end of annual growth and were used to fit each ring limitations.*

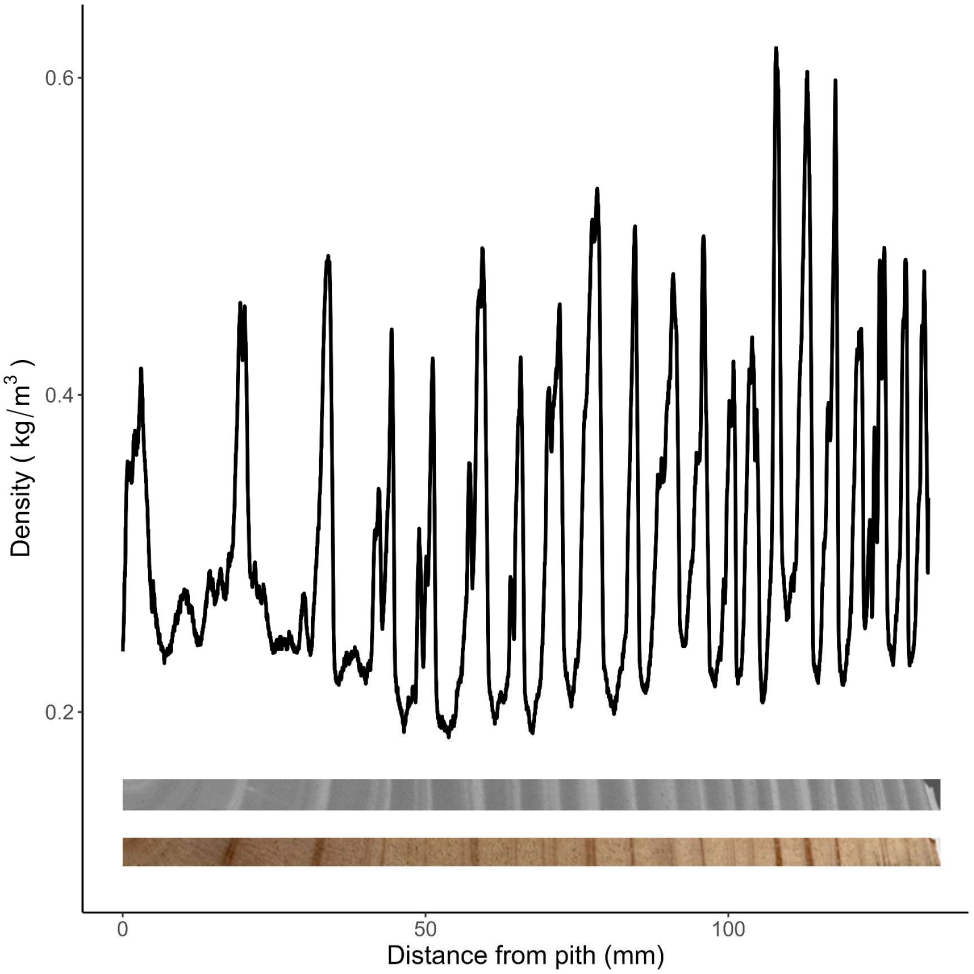

Figure 2: Cross-validation scenarios CV-A, CV-B, CV-C and CV-D performed with a RRM according to the GP' index. *All scenarios include the same amount of phenotypic information in the training set (i.e. 50% of total phenotypic data); only the distribution of this information across individuals and environmental levels differ. All families contributed equally to the training set.*

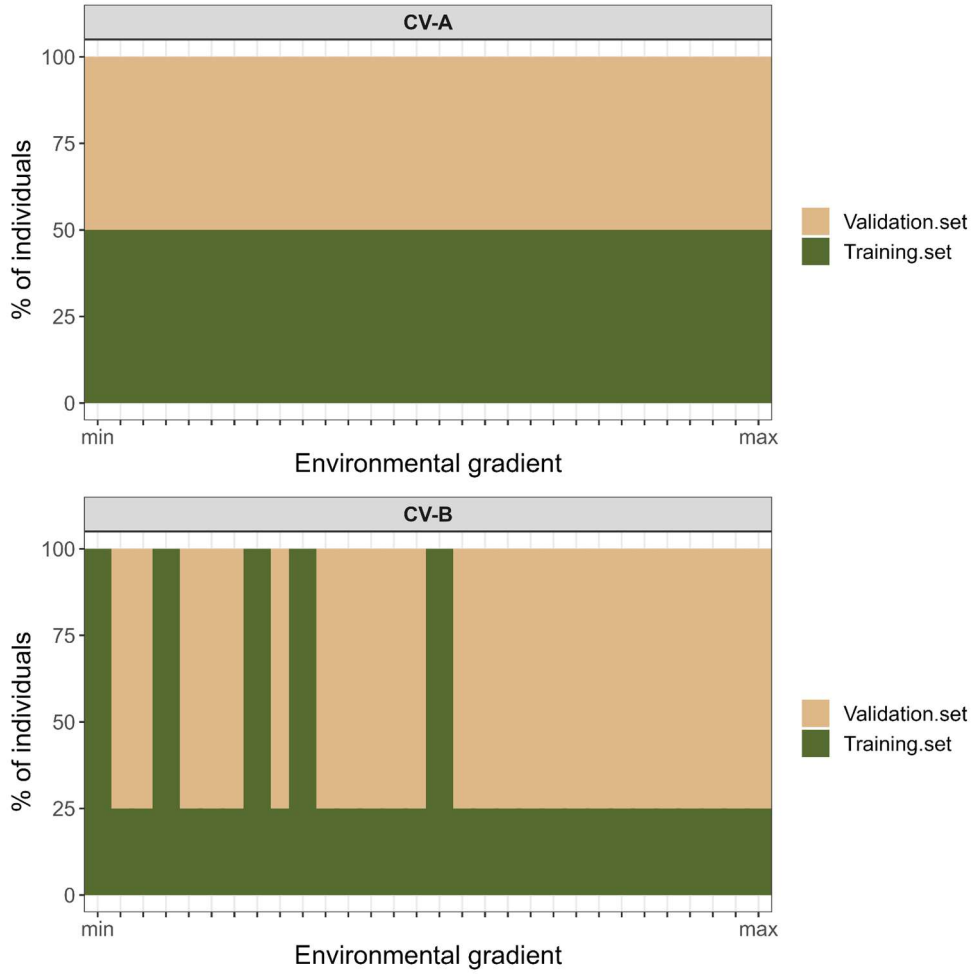

Figure 3: Comparison between pedigree-based additive relationship coefficients derived from pedigree and additive genomic relationship coefficients derived from SNP markers for individuals of POP. *For each value of the discrete scale taken by the pedigree-based additive relationship coefficients, the corresponding violin plot represents the continuous distribution of additive genomic relationship coefficients. Numbers below each violin plot denote the number of relationship included in the corresponding violin plot. Grey line is the bisector passing through the origin of the graph. The two highest pedigree-based additive relationship coefficients (1.25 and 1.5) are unique and so represented by single points instead of violin plots.*

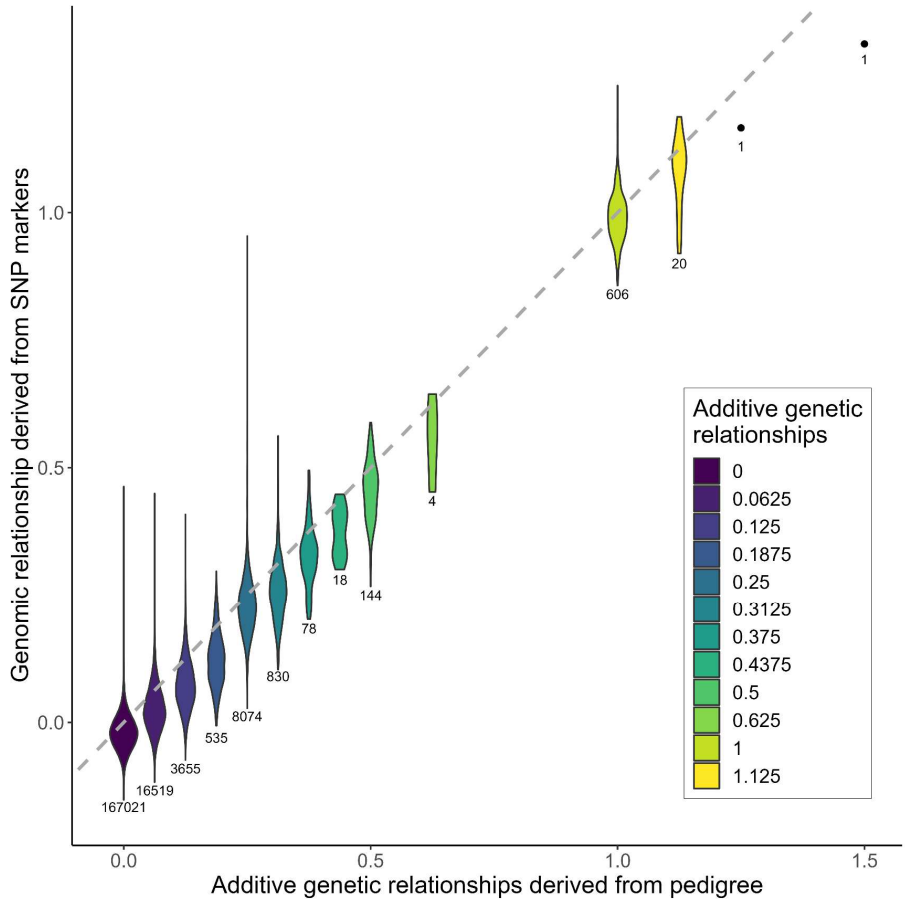

Figure 4: Prediction accuracy of the RRM according to the environmental gradient and the genetic information used. *Boxplots indicates the Pearson correlation coefficient between observed and predicted RA values over the whole environmental gradient for 10 repetitions of the CV-A scenario. Boxplots are blue when the RRM implemented integrated pedigree-based additive relationship coefficients while boxplots are yellow when the RRM implemented integrated additive genomic relationship coefficients. For each kind of genetic information, RRM were run independently with each of the four environmental gradients, respectively derived from* DM, DM', GP *and* GP' *indices.*

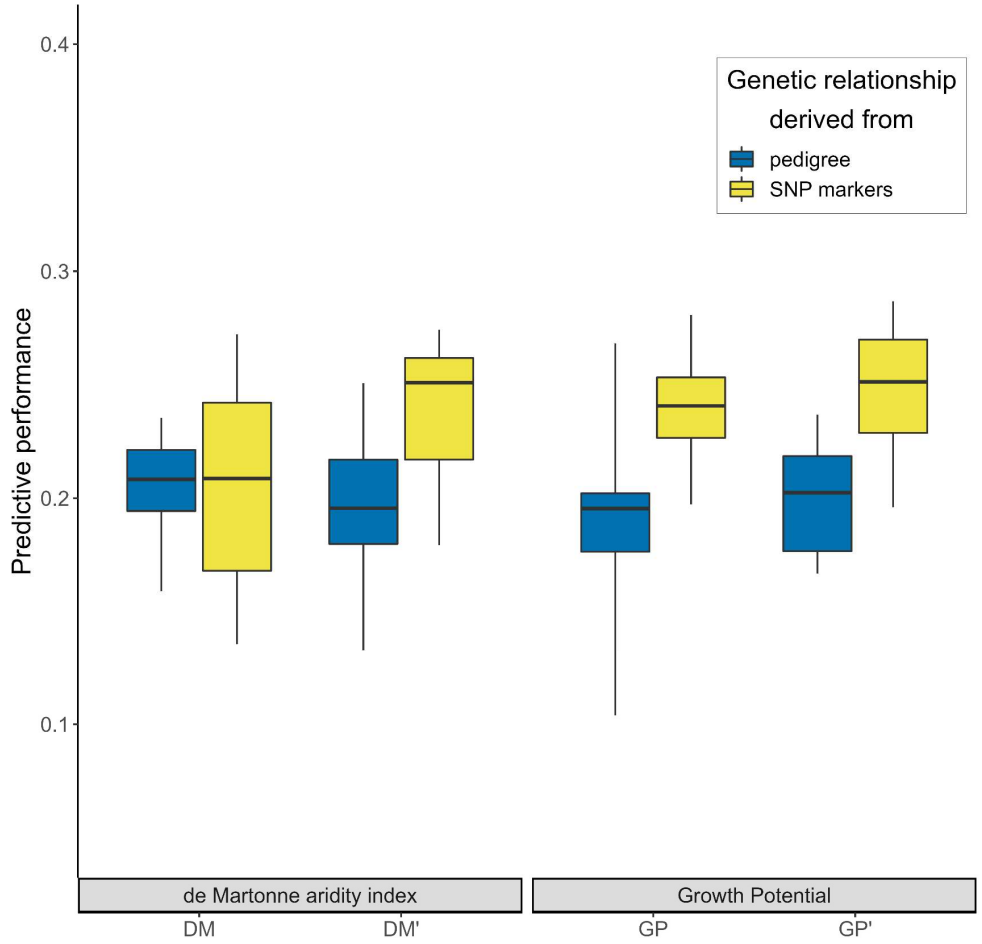

Figure 5: Evolution of mean RA according to the years for each site (Fig. 5A) or according to the GP' index (Fig. 5B). *Figure 5.A presents mean phenotypic trajectories of RA and Figure 5.B presents mean trajectories adjusted by the RRM for each site. Both trajectories are the result of the same model. The significance of the slope parameter for each trajectory in Figure 5.B was assessed with Student's t-test (p-value<0.01)*

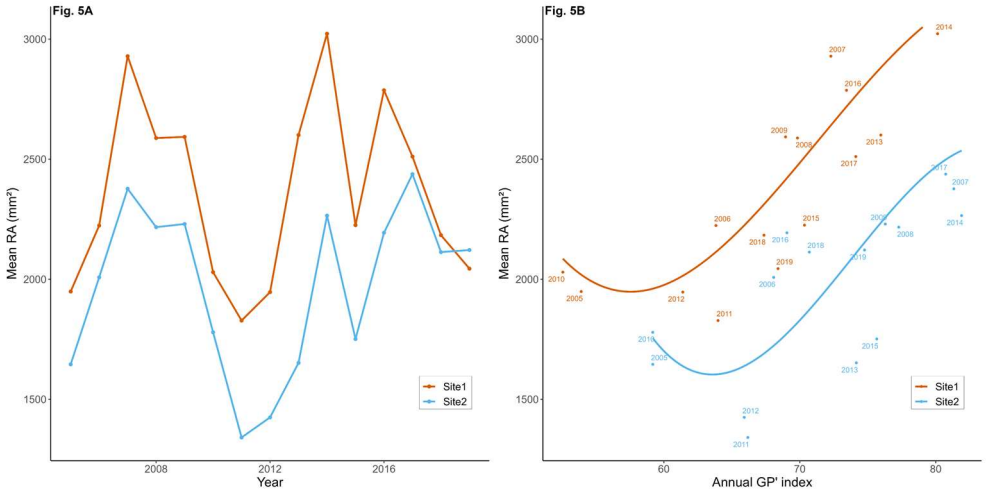

Figure 6: Individual trajectories of $GEBV_{ref}$ associated to RA according to the GP' index. *Trajectories correspond to the genetic component of the reaction norms estimated by the genomic based RRM. Trajectories were* colored according to their slope (quadratic regression coefficient), from the steepest negative slopes (dark red) to the steepest positive slopes (dark blue).

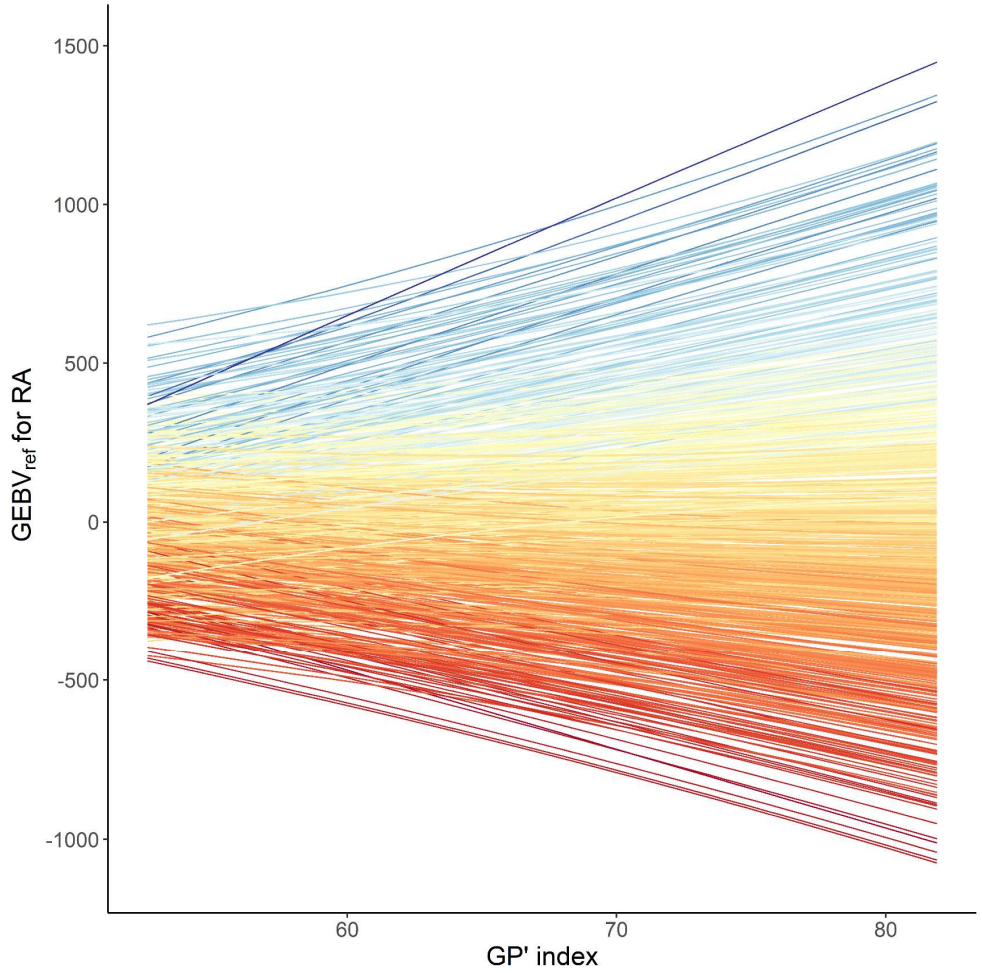

Figure 7: Maximum genetic gain (GG_{max}) and true genetic gain (GG_{true}) according to GP' index. *The RRM was used with complete phenotypic information for all individuals to estimate $GEBV_{ref}$ over the gradient; and then independently repeated 10 times with the scenario CV-A to predict $GEBV_{pred}$ for individuals in the validation set. GG_{max} was calculated as the mean of the top 5% of $GEBV_{ref}$ and for each iteration GG_{true} was calculated as the mean of $GEBV_{ref}$ associated to the top 5% individuals selected based on $GEBV_{pred}$ for each GP' values. GG_{max} and GG_{true} are centered and reduced.*

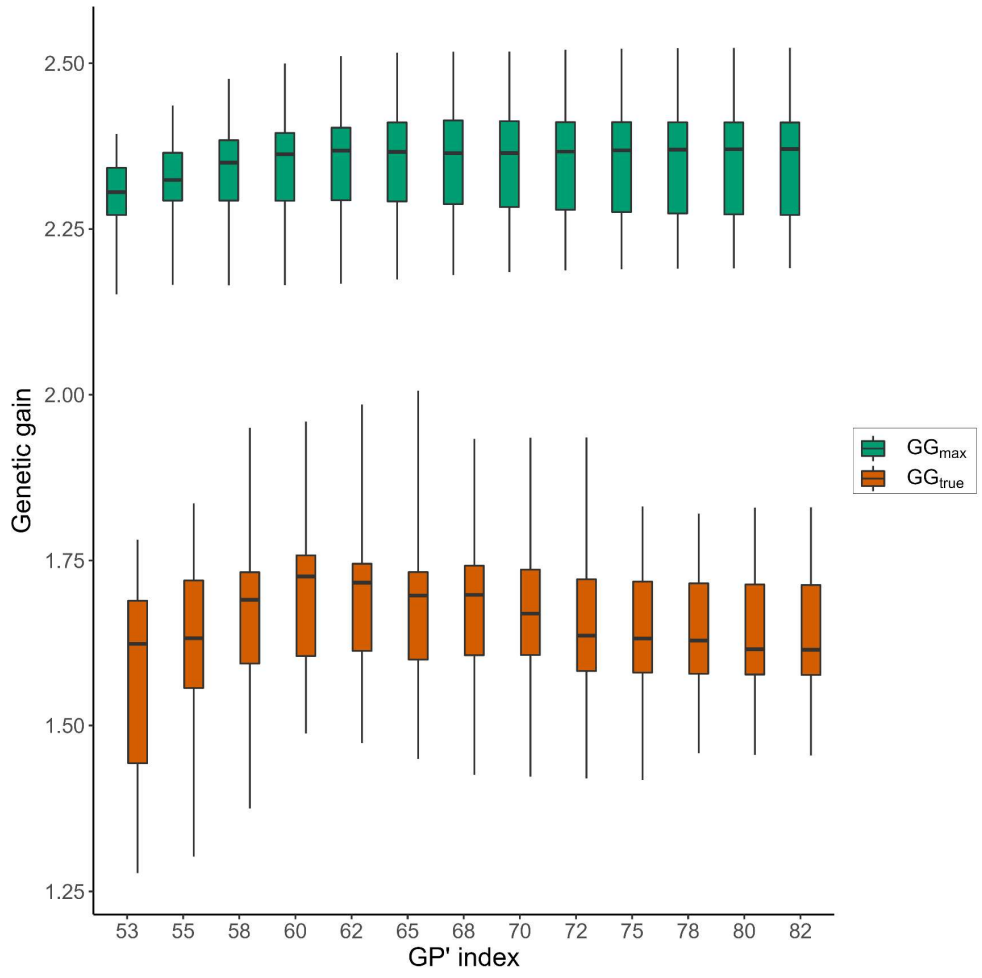

Figure 8: Prediction accuracy of the RRM according to the CV-A and CV-B scenarios. *Boxplots indicates the Pearson correlation coefficient between observed and predicted RA values over the whole environmental gradient for 10 independent repetitions of the CV scenario. The significance between prediction accuracies was assessed by a Student's t-test (****: p-value <1e10-4)*